ICIFMS-19
ROMA 2022

19th International Conference on Internal Friction and Mechanical Spectroscopy

Lattice dynamics in niobium doped $PbZrO_3$ single crystals

Dariusz Kajewski

Rome, Italy, 28th of June 2022

An international team

- Institute of Physics, University of Silesia, Chorzów, Poland
  K. Roleder, A. Soszyński, J. Koperski, D. Kajewski
- School of Nano Convergence Technology, Nano Convergence Technology Center, Hallym University, Chuncheon 24252, Korea
  J.H. Ko, B. Lee, S. Oh
- Institute of Physics, Pedagogical University, ul. Podchorążych 2, Kraków, Poland
  I. Jankowska-Sumara
- Max-Planck-Institut für Festkörperforschung, Heisenbergstrasse 1, D-70569 Stuttgart, Germany
  A. Bussmann-Holder
- Institute of Applied Physics, Military University of Technology, ul. Kaliskiego 2, 00–908 Warsaw, Poland
  A. Majchrowski

$PbZrO_3$ - Well known and unknown

- Known since 1950 (G. Shirane, E. Sawaguchi, and A. Takeda, Phys. Rev. **80**, 485 (1950))

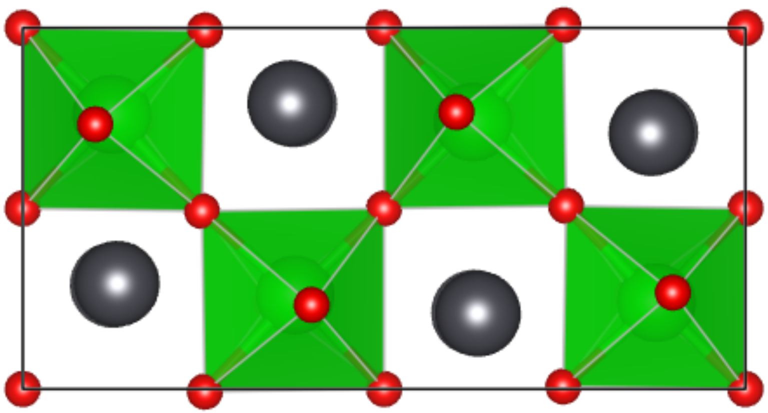

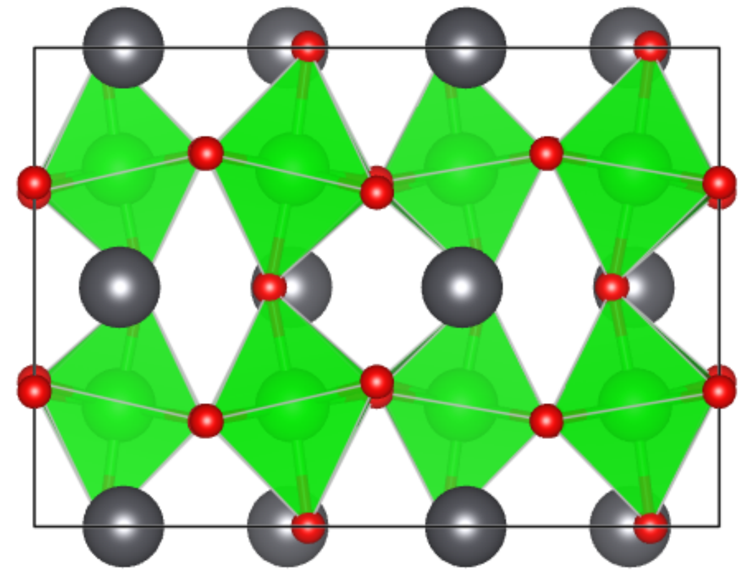

$PbZrO_3$ - Well known and unknown

- Still not very well known from the phase transitions mechanism point of view.

Bussmann-Holder, A., Ko, J.-H., Majchrowski, A., Górny, M., & Roleder, K. (2013). *Precursor dynamics, incipient ferroelectricity and huge anharmonicity in antiferroelectric lead zirconate $PbZrO_3$. Journal of Physics: Condensed Matter, 25(21), 212202.*

- It is known that defects influence properties of $PbZrO_3$ such as phase transitions, electrical properties…

D. Kajewski, J. Kubacki, K. Balin, I. Lazar, J. Piecha, A. Bussmann-Holder, J.-H. Ko, K. Roleder, Defect-induced intermediate phase appearance in a single $PbZrO_3$ crystal, J. Alloys and Comp. 812 (2020)152090

- Niobium is heterovalent dopant creating or compensating lead defects.

D. Kajewski, J. Kubacki, A. Bussmann-Holder, K. Roleder, Surface–bulk interrelation in a $PbZrO_3$ single crystal, J. Mat. Chem. C 5, 2017, pp. 10456-10461

Lead zirconate ceramics doped with Nb

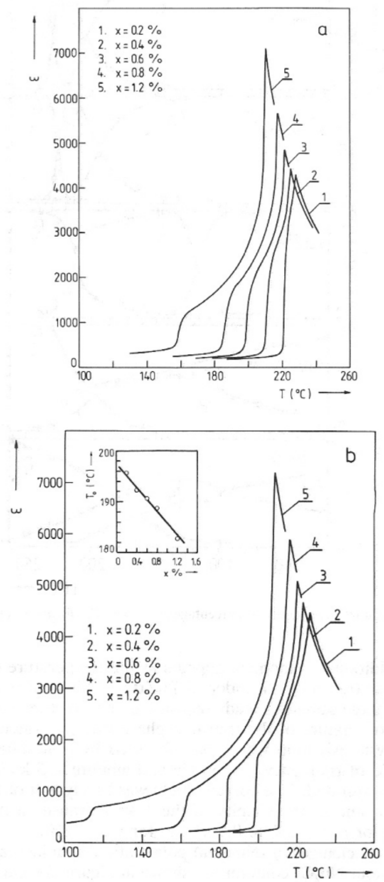

FIGURE 4 Temperature dependences of permittivity on heating (a) and cooling (b) and variation of the Curie-Weiss temperature T_O with Nb_2O_5 content (b).

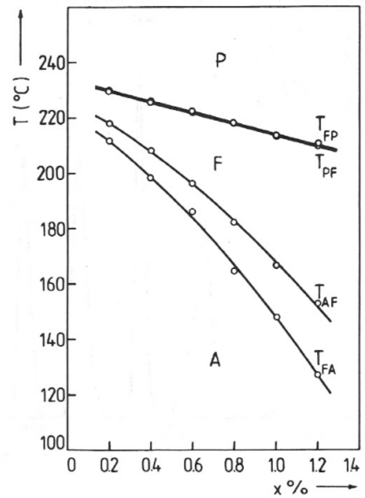

FIGURE 7 Variation of phase transitions temperatures versus Nb_2O_5 content.

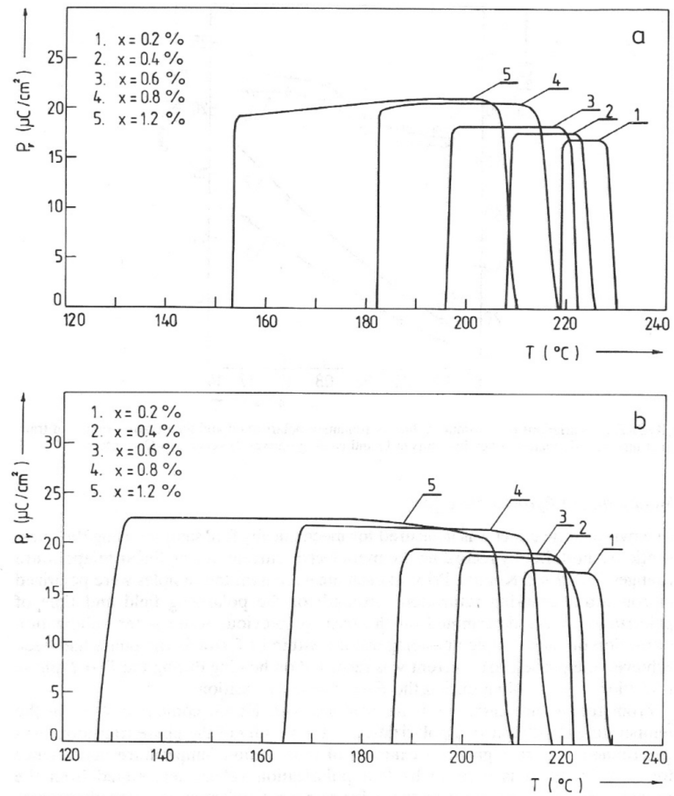

FIGURE 5 Temperature dependences of remanent polarization on heating (a) and cooling (b).

Z. Ujma et. al., Structure and electrical properties of $PbZrO_3$ doped with Nb_2O_5, Ferroelectrics 120 (1991) 211

Unexpected phase transitions in PZO:Nb single crystals

Nominal Nb_2O_5 concentration: 1.0 mol% (from ceramics)

Nominal Nb_2O_5 concentration: 1.0 mol%

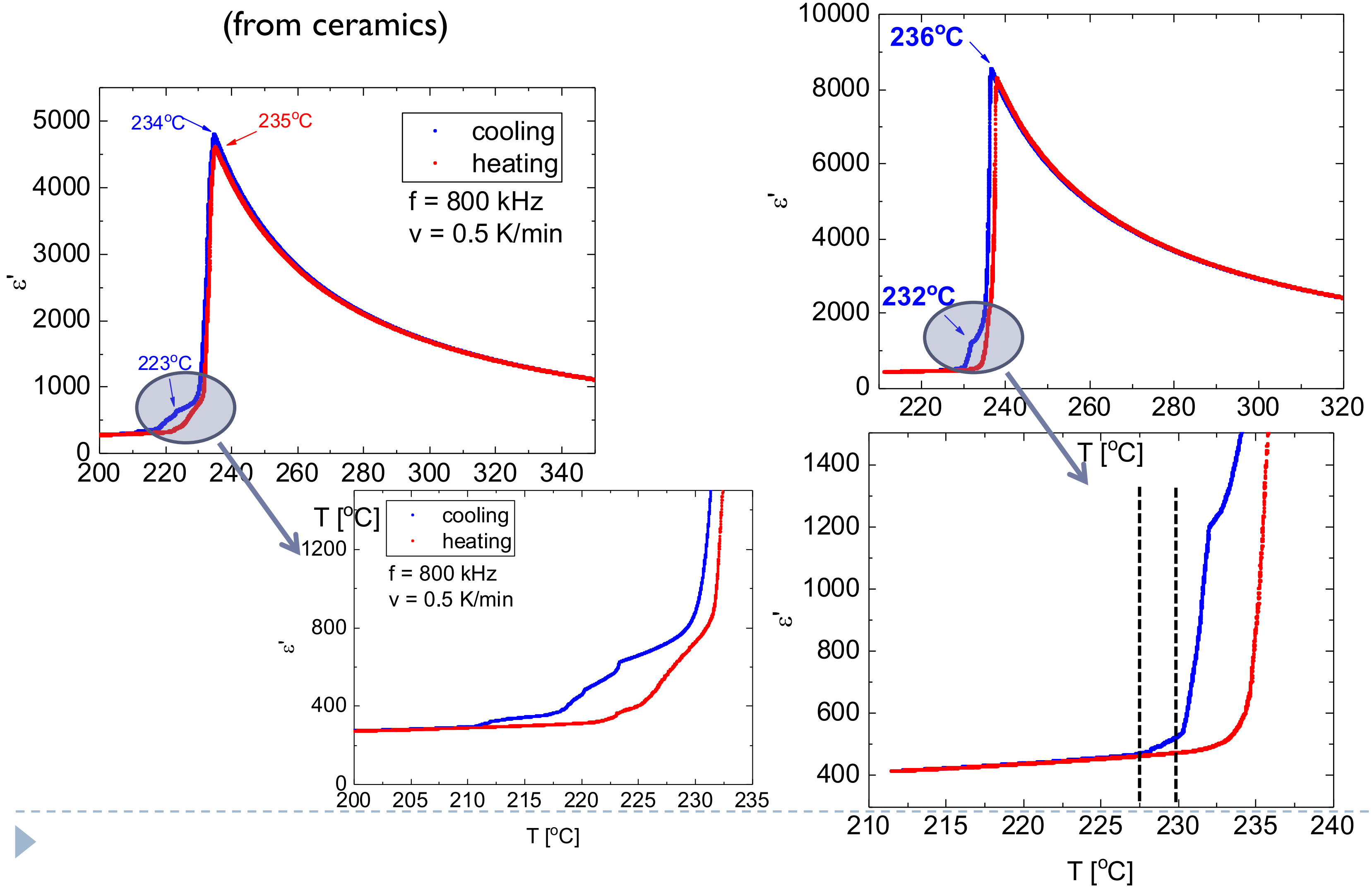

Optical properties of PZO:1.0 mol%Nb_2O_5

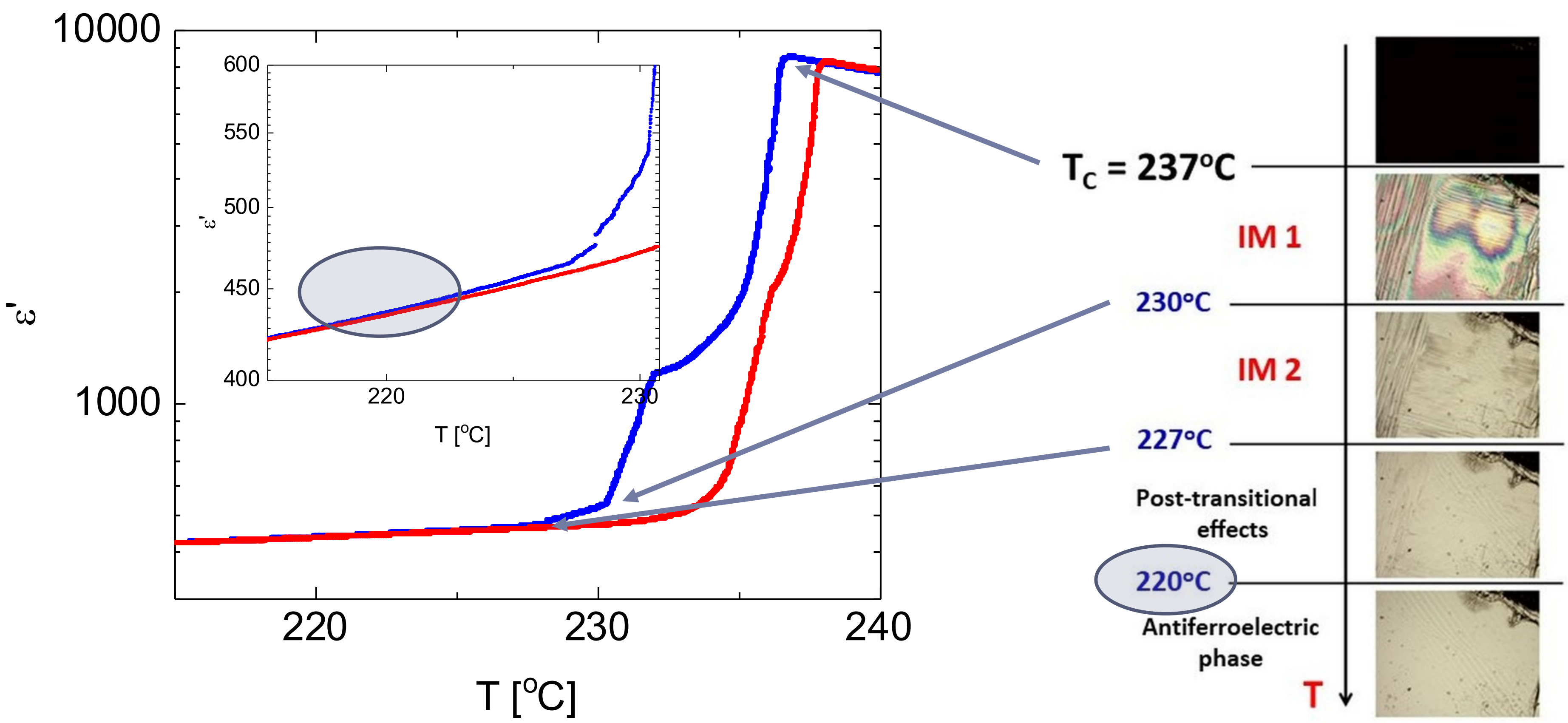

D. Kajewski et al. J Am Ceram Soc. 2020;103:3657–3666.

Pre-transitional effects

$$\Delta T = 1.1 \cdot T_C - T_C = [1.1 \cdot (237+273.16)]-(237+273.16) = 51K$$

Theoretical predictions:
***„Precursor effects, broken local symmetry and coexistence of order disorder and displacive dynamics in perovskite ferroelectrics"* by**
A. Bussmann-Holder et *al.*
Phys. Rev. <u>B79</u>, 184111, 2009

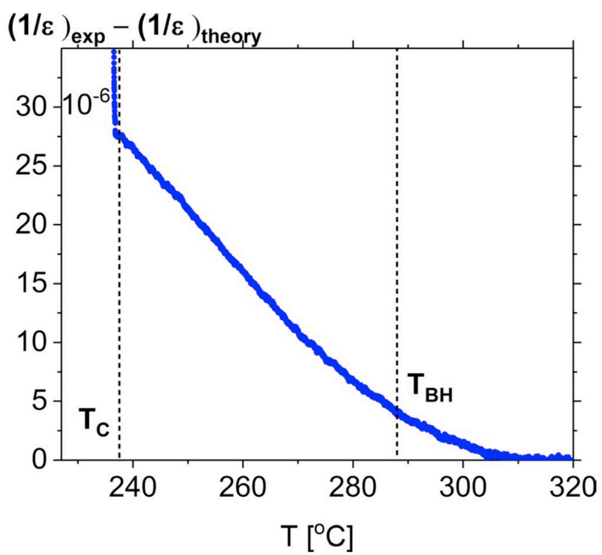

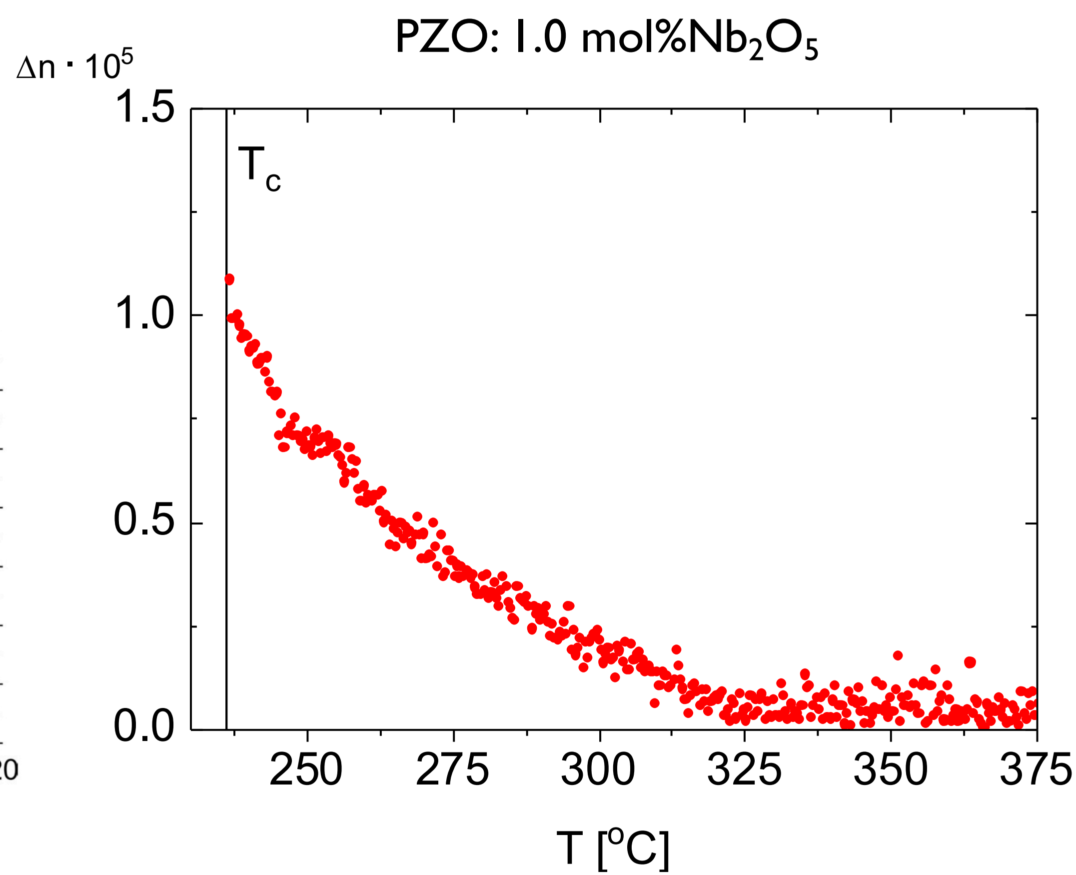

D. Kajewski et al. J Am Ceram Soc. 2020;103:3657–3666.

New phase transition?

- Observed in:
- dielectric properties
- optical properties
- specific heat changes

of crystals from two different technologies

- Reversible and repeatable

?

Raman scattering in PZO:Nb

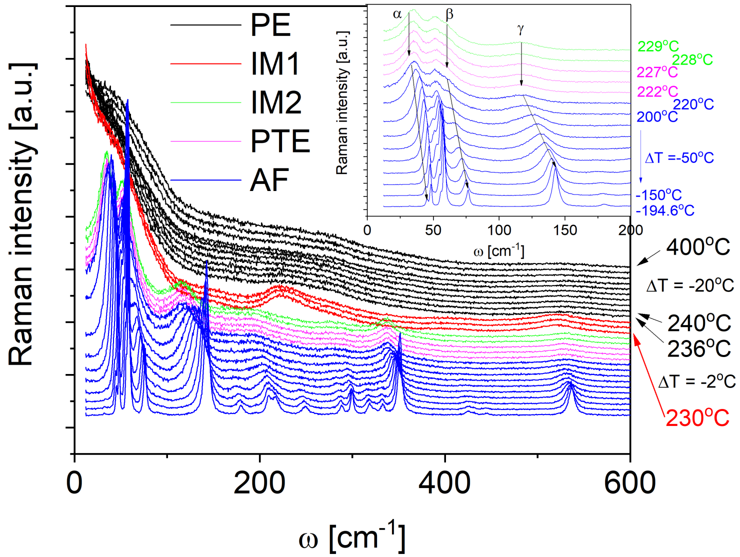

$$I_R(\omega) = \begin{Bmatrix} n(\omega)+1 \\ n(\omega) \end{Bmatrix} \left(\frac{S_r \gamma_r \omega}{\omega^2 + \gamma_r^2} + \sum_i \frac{S_i \omega_i^2 \gamma_i \omega}{\left(\omega_i^2 - \omega^2\right)^2 + \gamma_i^2 \omega^2} \right)$$

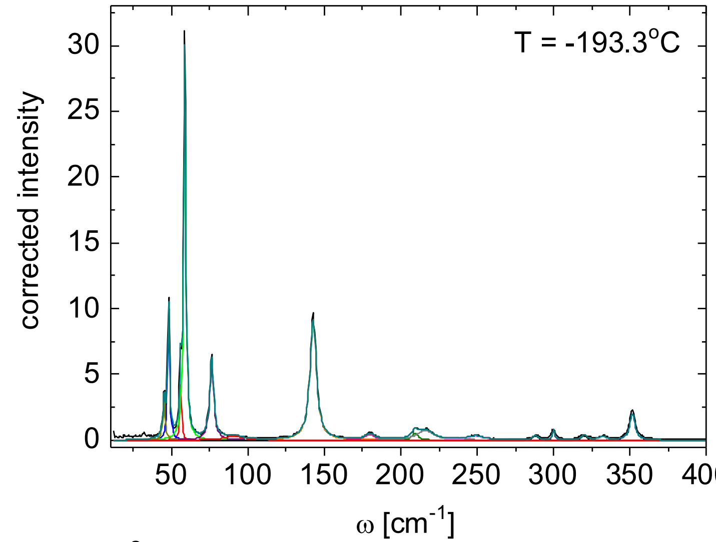

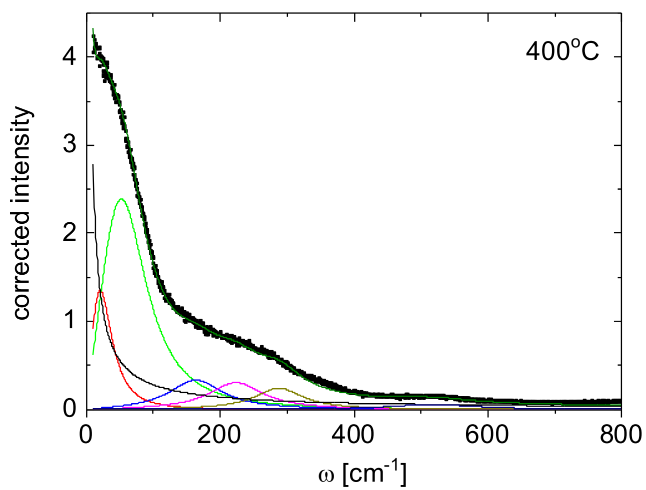

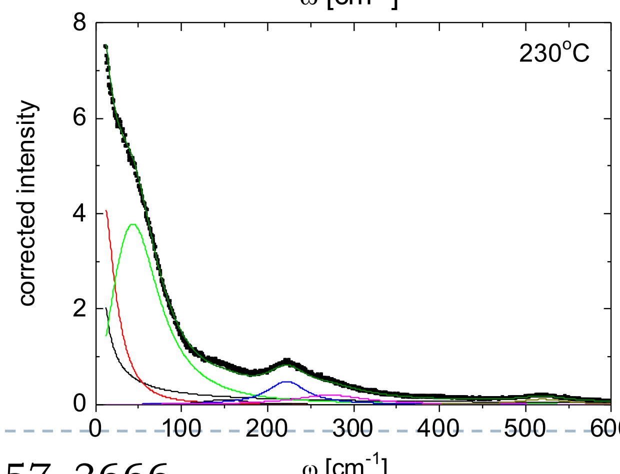

D. Kajewski et al. J Am Ceram Soc. 2020;103:3657–3666.

Raman scattering in PZO:Nb

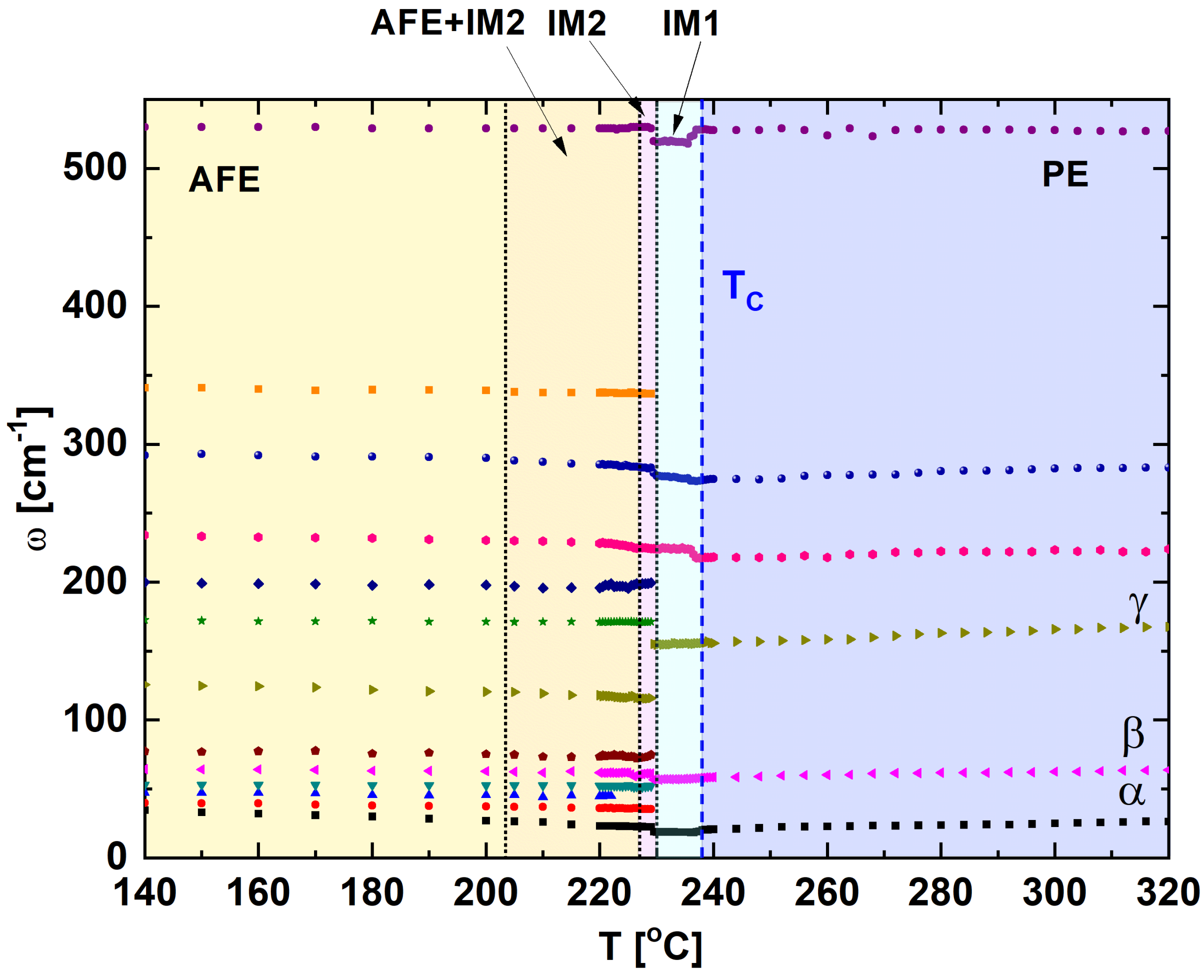

D. Kajewski et al. J Am Ceram Soc. 2020;103:3657–3666.

Raman scattering in PZO:Nb

Antiphase oxygen octaheadra tilts and lead ions

Cochran's law $\omega^2 \sim (T - T_c)$ 3 soft modes!

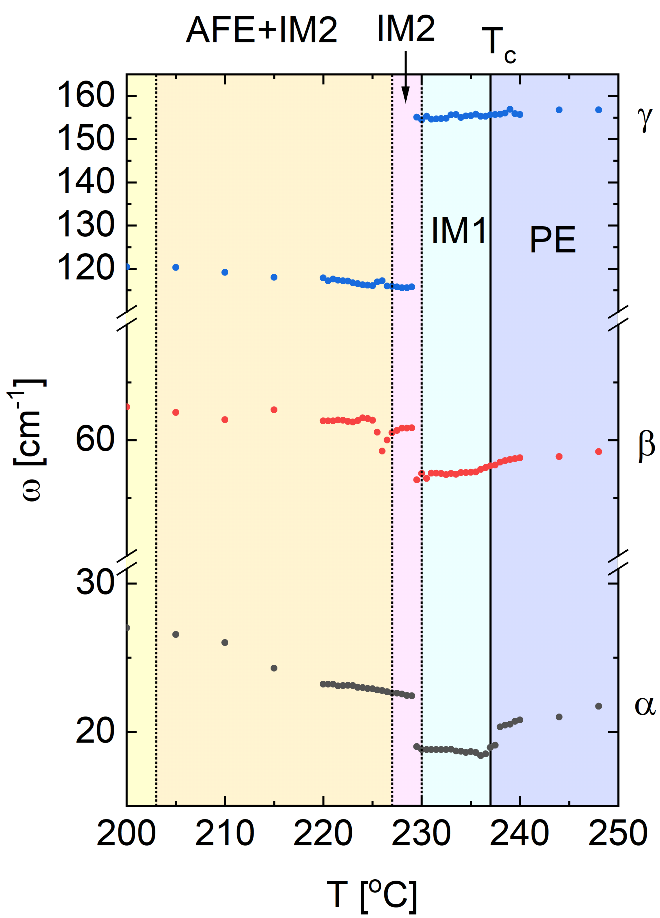

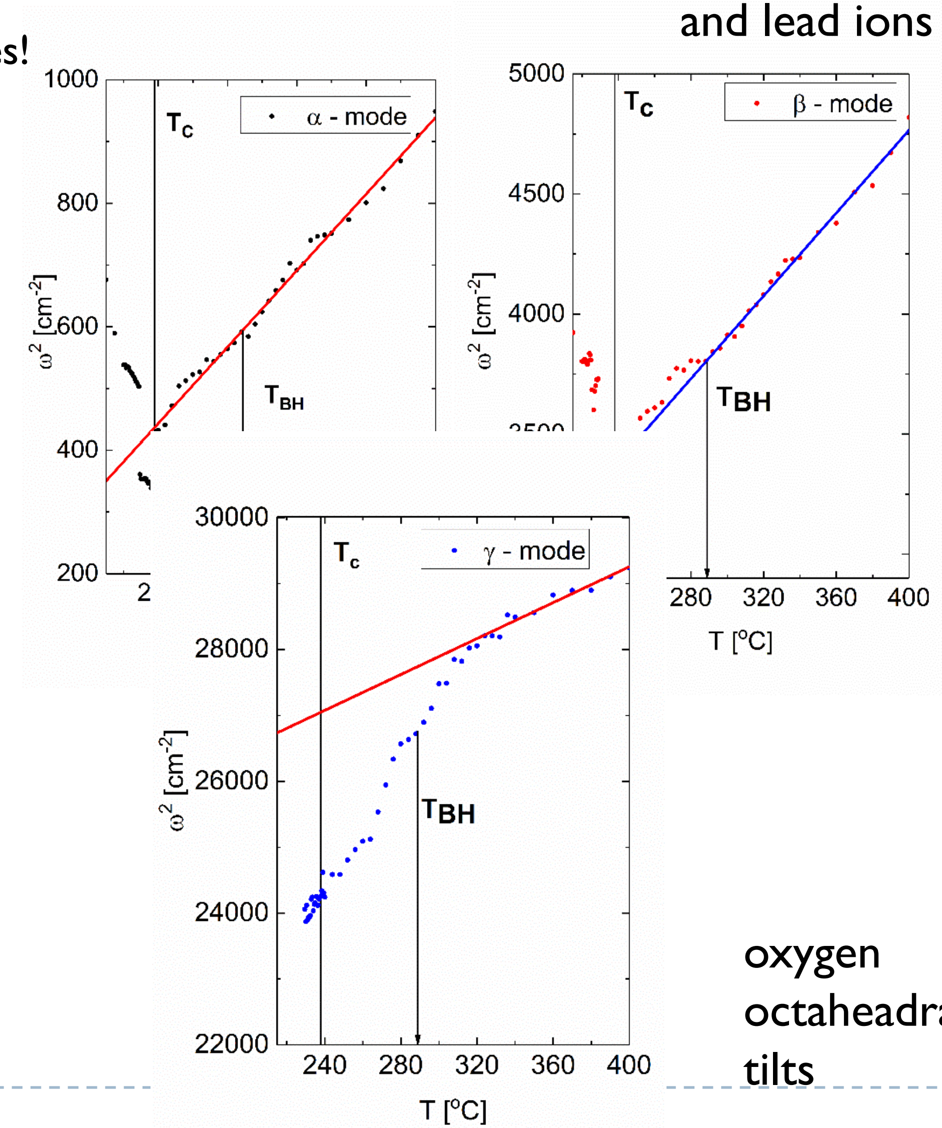

oxygen octaheadra tilts

D. Kajewski et al. J Am Ceram Soc. 2020;103:3657–3666.

Raman scattering

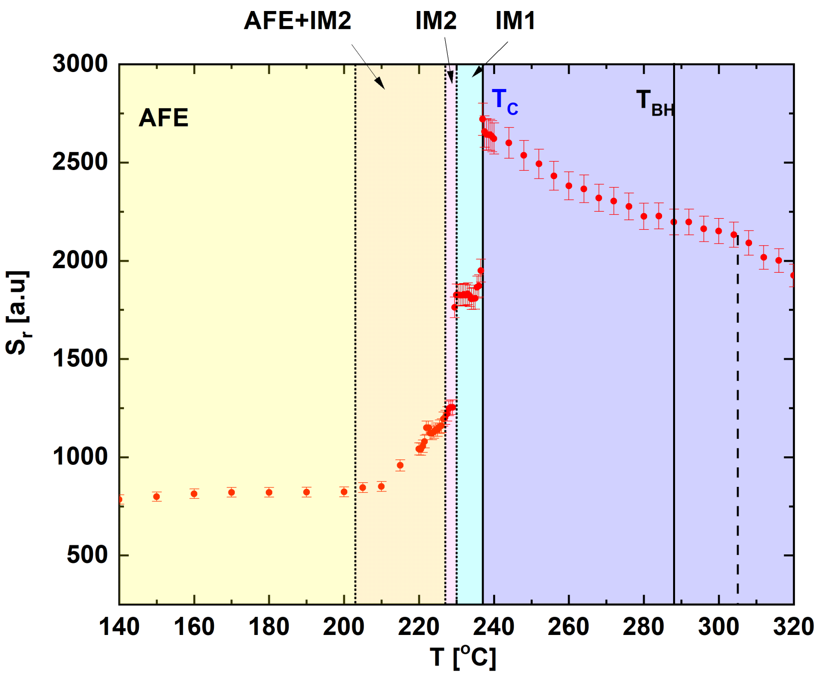

CP from strong relaxational motion of Pb
in the A position

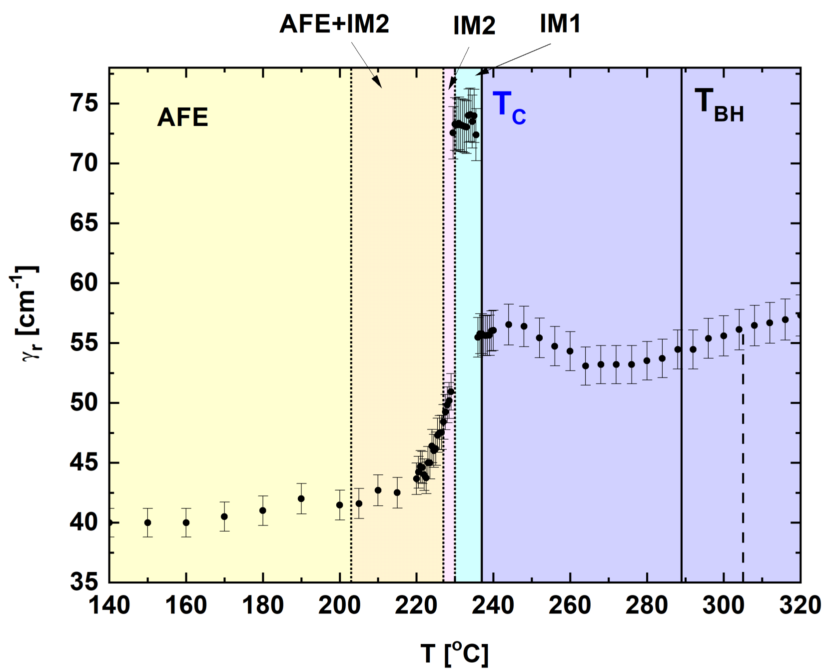

D. Kajewski et al. J Am Ceram Soc. 2020;103:3657–3666.

Brillouin scattering

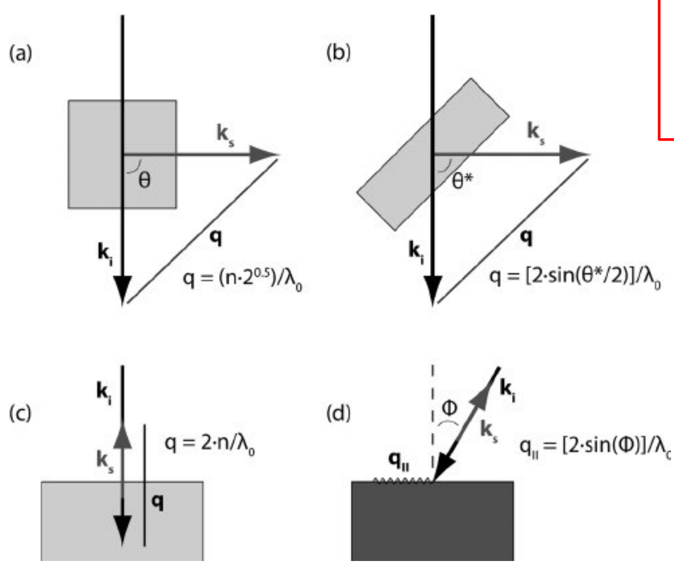

(a) 90° normal geometry; (b) forward symmetric geometry (here refraction is not taken into account and θ * is the external scattering angle; (c) 180° backscattering geometry; (d) tilted backscattering geometry for surface Brillouin scattering measurements.

PHYSICAL REVIEW B VOLUME 6, NUMBER 2 15 JULY 1972

Brillouin Scattering: A Tool for the Measurement of Elastic and Photoelastic Constants

R. Vacher and L. Boyer

Laboratoire de Physique de l'Etat Cristallin, Université des Sciences et Techniques du Languedoc, 34 Montpellier, France

(Received 26 August 1970)

$$\rho \ddot{U}_i = C_{ijkl} \frac{\partial^2 U_l}{\partial x_j \partial x_k}$$

$$\gamma U_i = \Gamma_{il} U_l$$

$$\gamma = \rho V^2$$

$$\Gamma_{il} = C_{ijkl} Q_j Q_k$$

$$V = \frac{\Delta\omega}{q}$$

U – displacement of an elemental volume of density ρ

C_{ijkl} – the components of the tensor of the elastic constants

- Speziale, Sergio & Marquardt, Hauke & Duffy, Thomas. (2014). Brillouin Scattering and its Application in Geosciences. Reviews in Mineralogy and Geochemistry. 78. 543-603

Brillouin scattering - backscattering

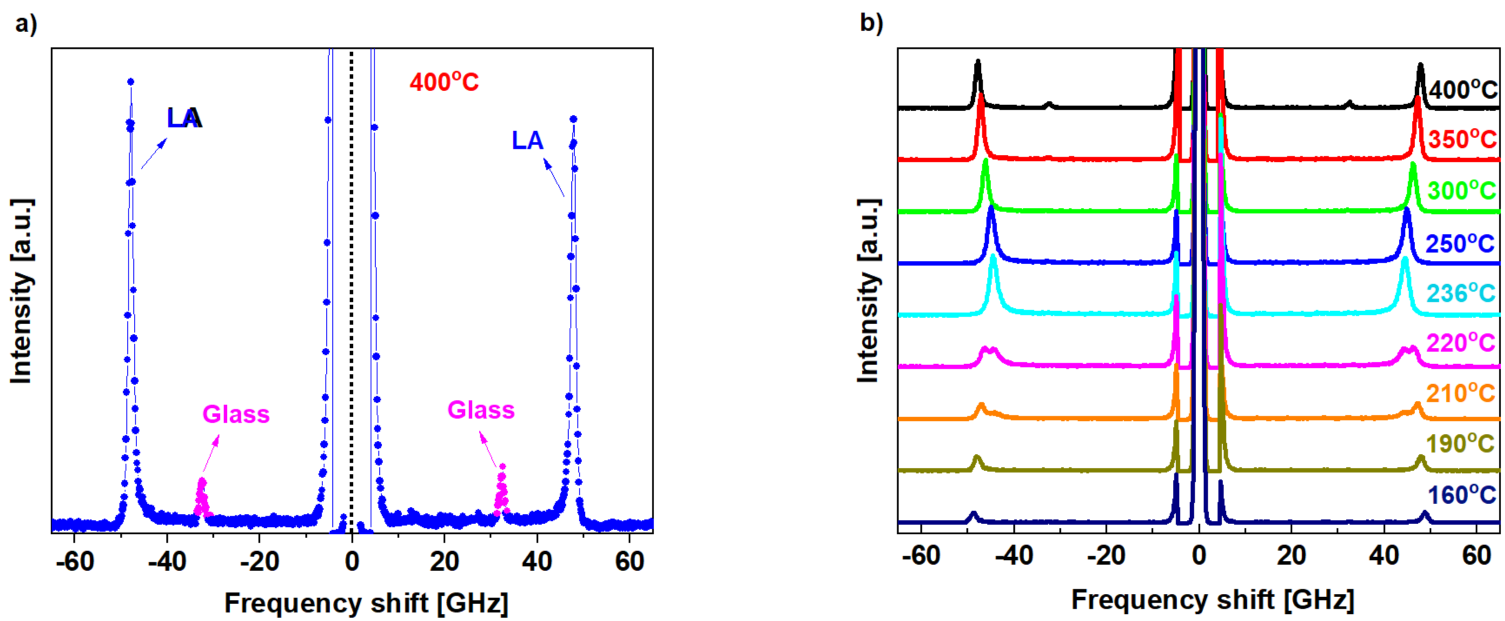

Only longitudinal acoustic mode could be observed

Brillouin scattering - backscattering

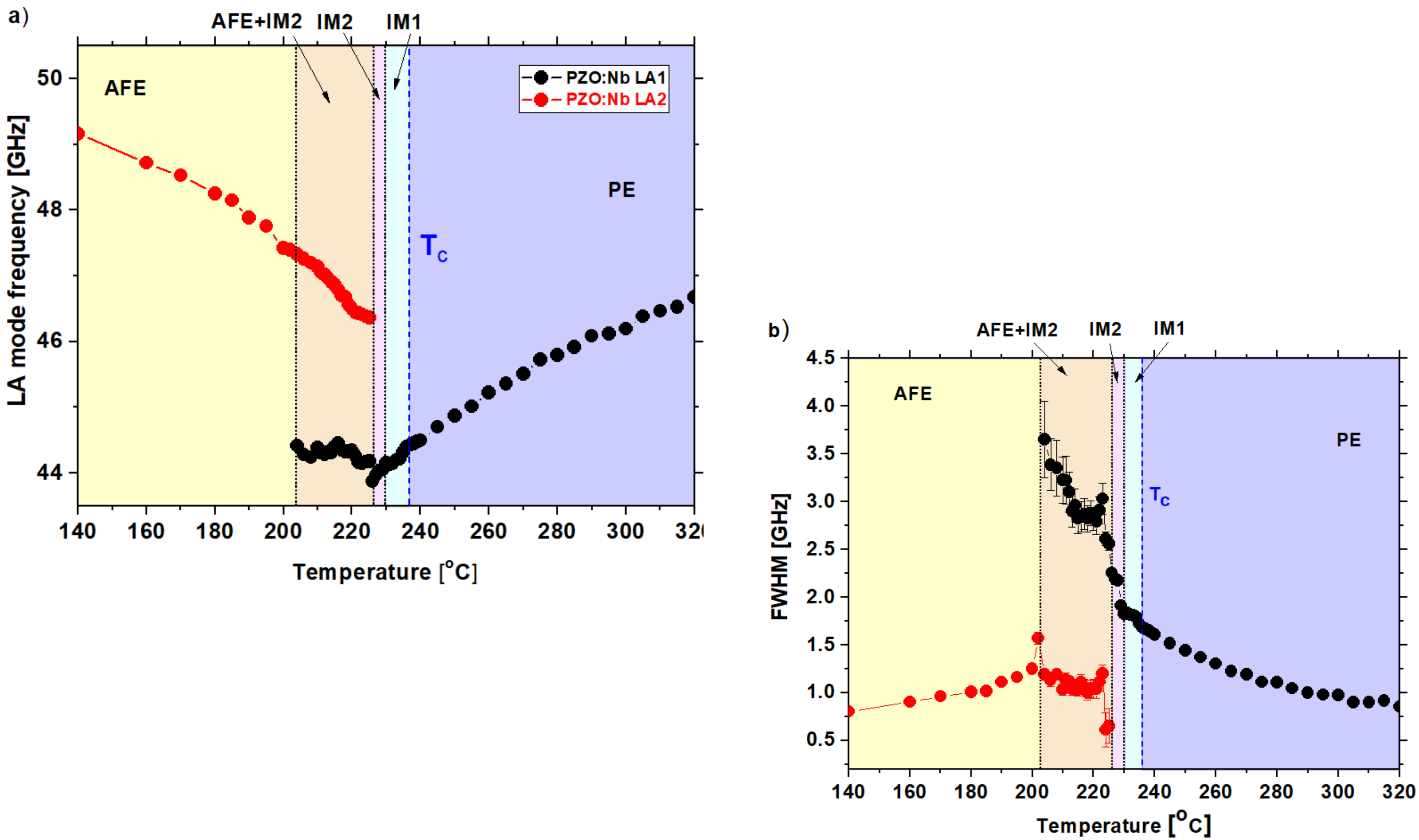

Brillouin scattering - backscattering

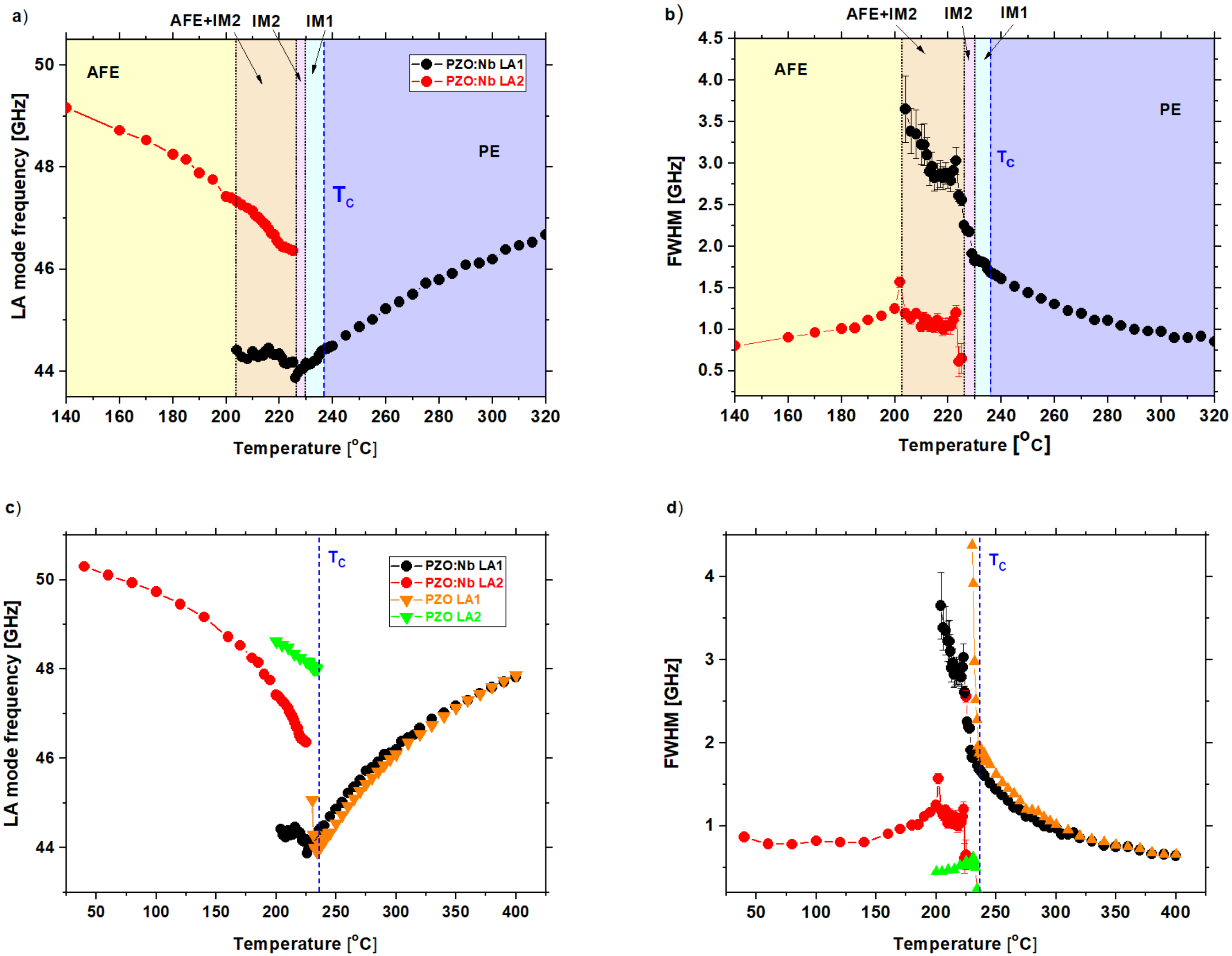

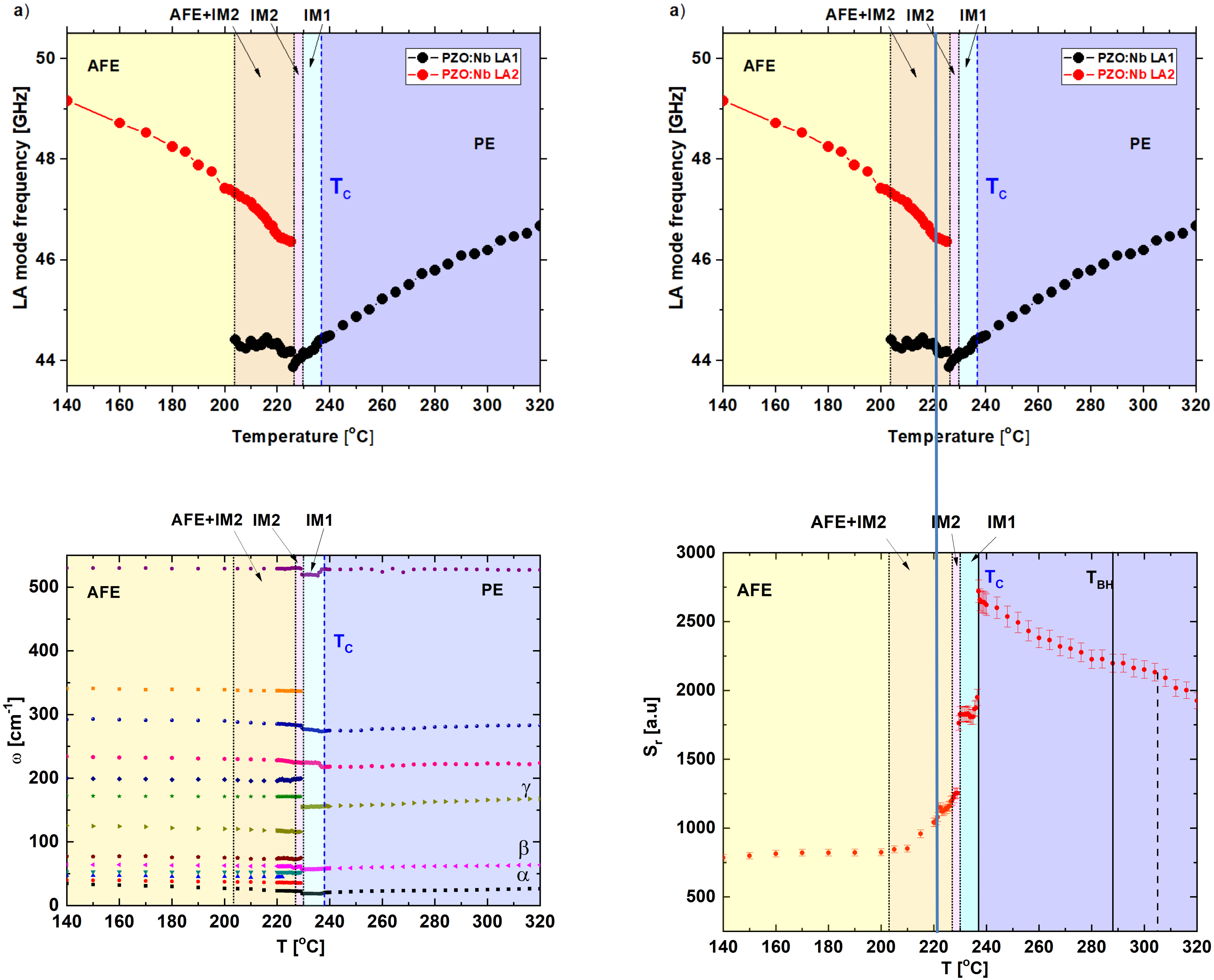

a)
AFE+IM2
IM2
IM1
AFE
PE
T_C
PZO:Nb LA1
PZO:Nb LA2
LA mode frequency [GHz]
Temperature [°C]
a)
AFE+IM2
IM2
IM1
AFE
PE
T_C
PZO:Nb LA1
PZO:Nb LA2
LA mode frequency [GHz]
Temperature [°C]
AFE+IM2
IM2
IM1
AFE
PE
T_C
γ
β
α
ω [cm⁻¹]
T [°C]
AFE+IM2
IM2
IM1
AFE
T_C
T_{BH}
S_r [a.u]
T [°C]

Brillouin scattering - backscattering

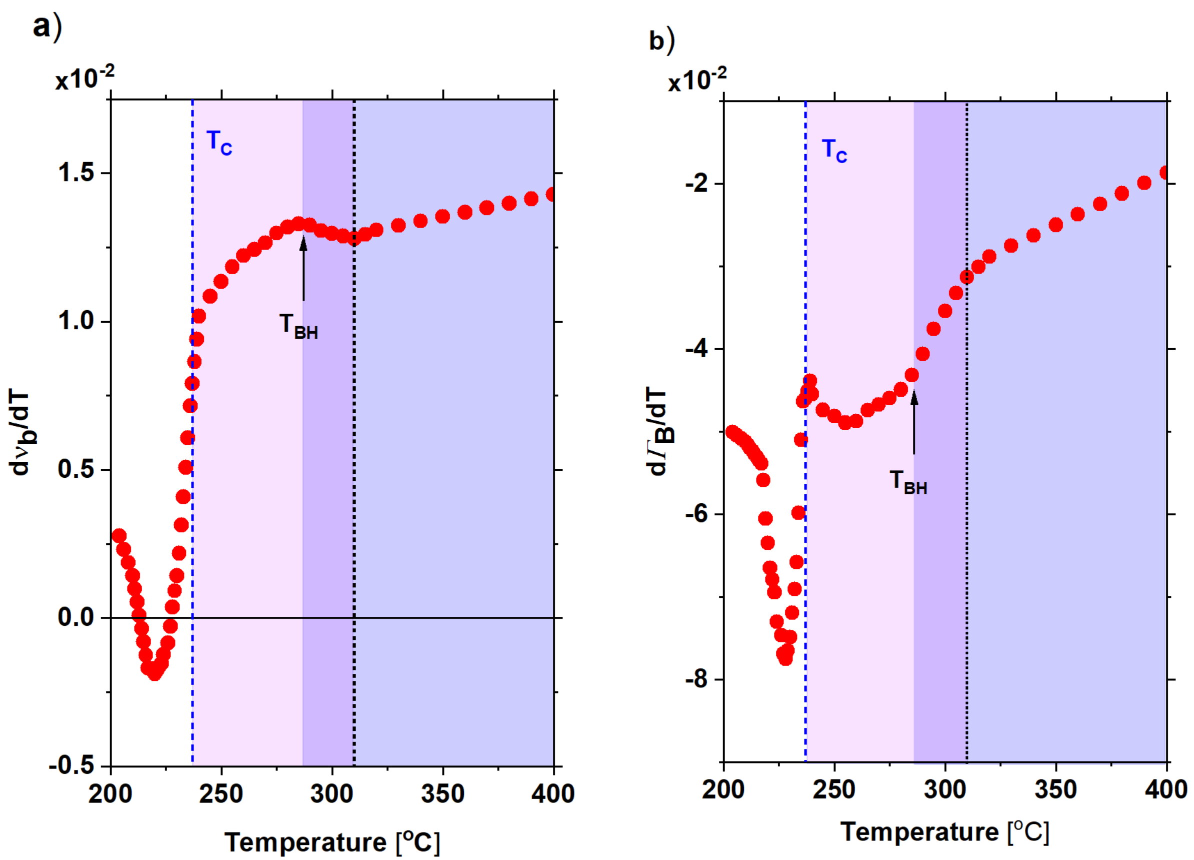

Brillouin scattering - backscattering

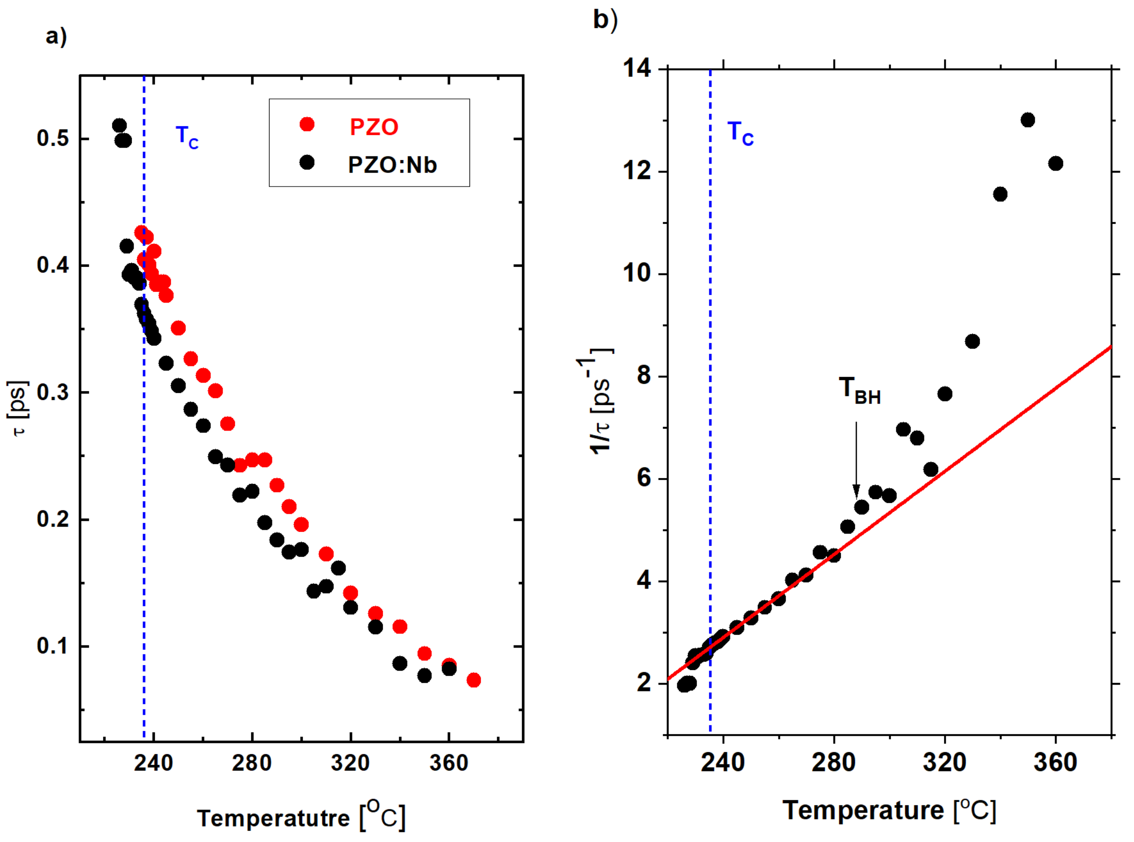

Brillouin scattering - forward symmetric geometry

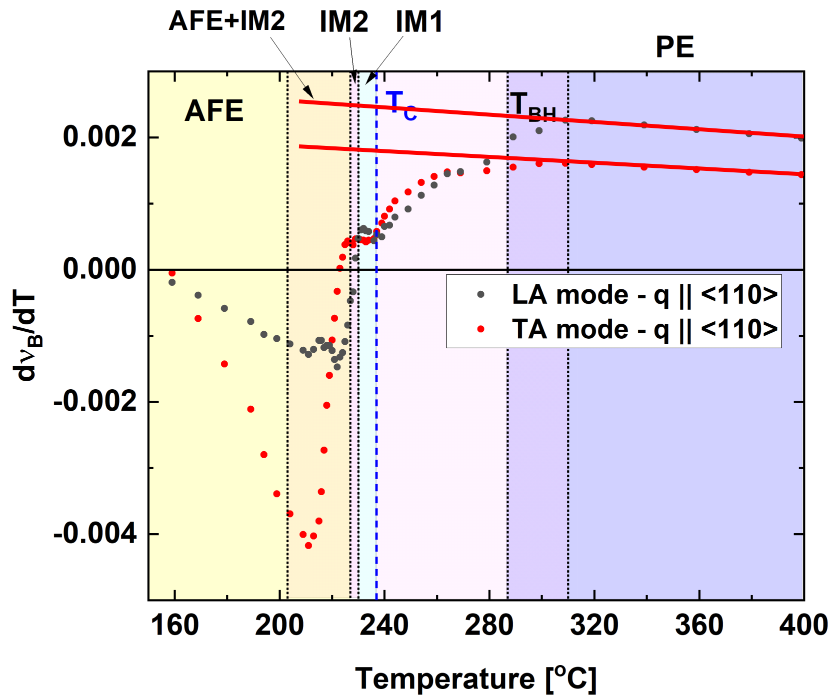

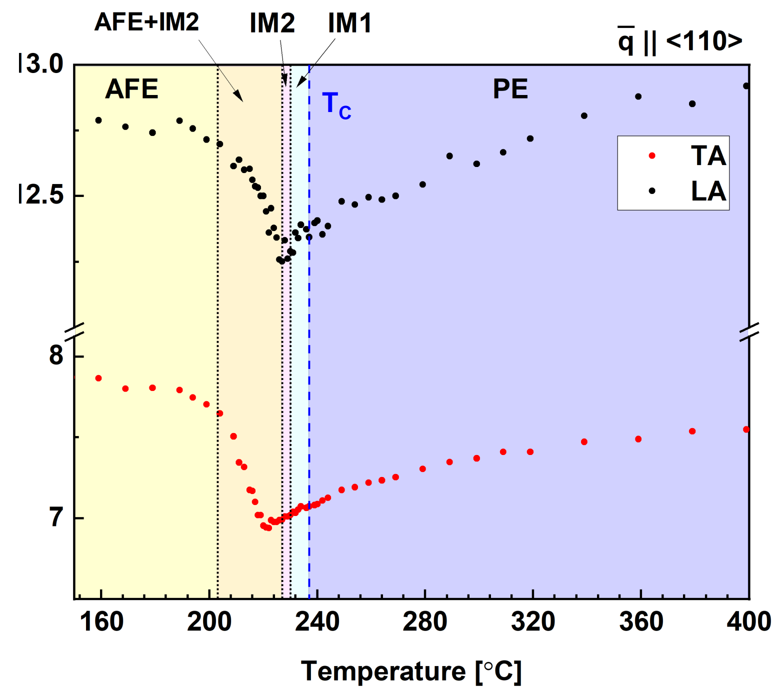

Wavevector	LA mode	TA mode
q ‖ <100>	C_{11}	C_{44} (doubly degenerate)
q ‖ <110>	$(C_{11}+C_{12}+2C_{44})/2$	$(C_{11}-C_{12})/2$ and/or C_{44}

Vacher R and Boyer L 1972 Phys. Rev. B 6 639

Brillouin scattering - forward symmetric geometry

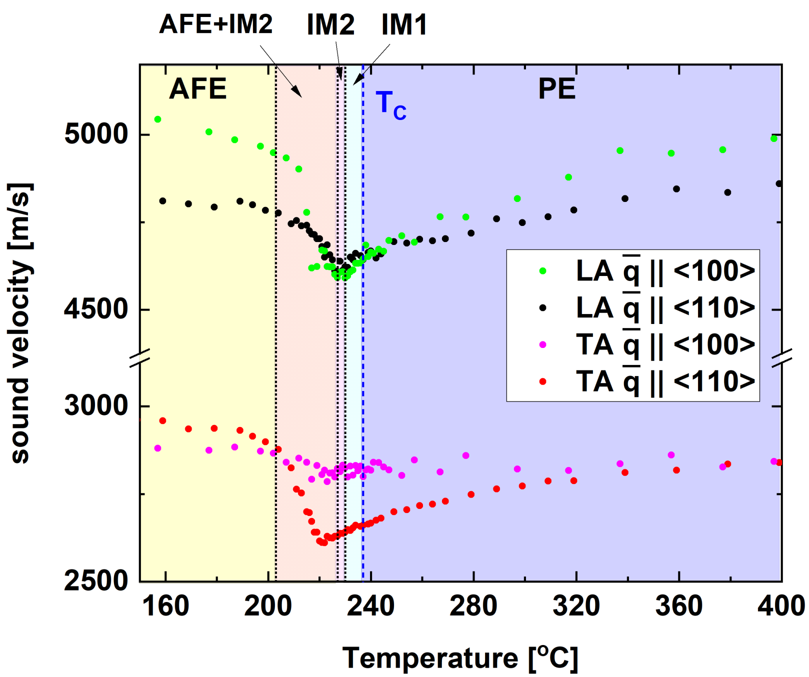

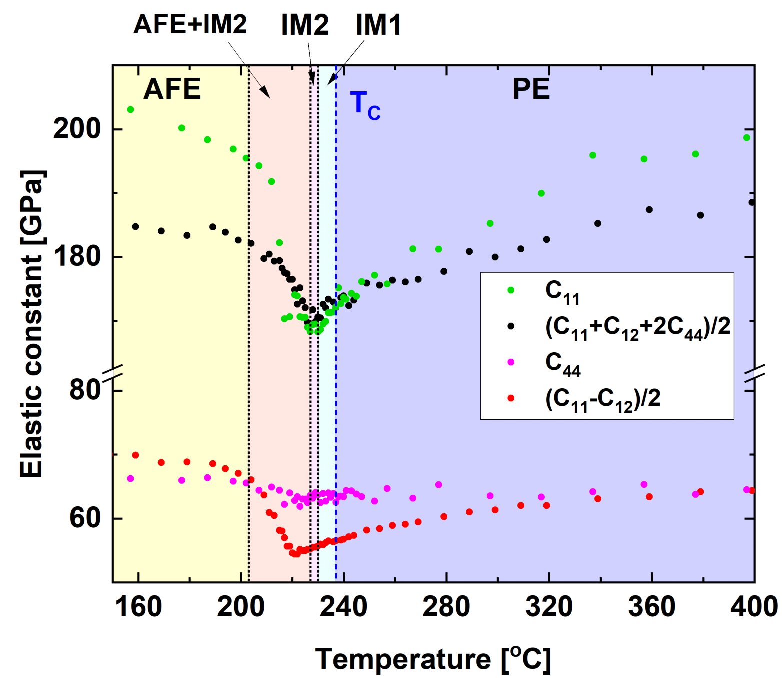

three symmetrized elastic constants in the cubic phase: $C_{11}+2C_{12}$, $(C_{11}-C_{12})/2$ and C_{44}
These three constants are related to the acoustic instabilities of the hydrostatic, tetragonal or orthorhombic, and rhombohedral deformation in sequence

J H Ko et al IOP Conf. Series: Materials Science and Engineering 54 (2014) 012002

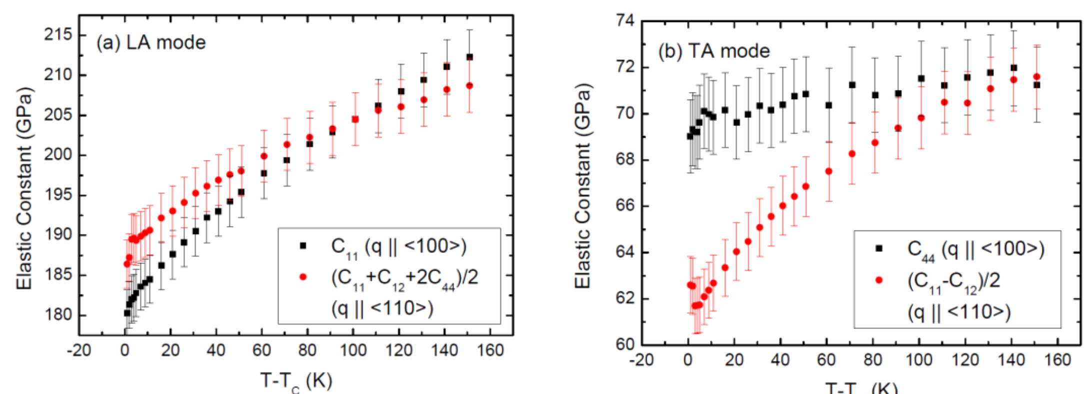

Figure 3. Temperature dependence of the elastic constants obtained from the LA and TA mode behaviors. (See Ref. [19])

Brillouin scattering - forward symmetric geometry

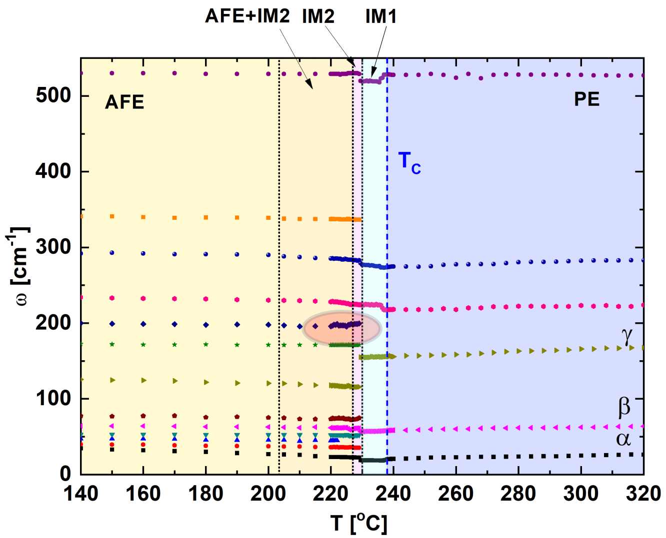

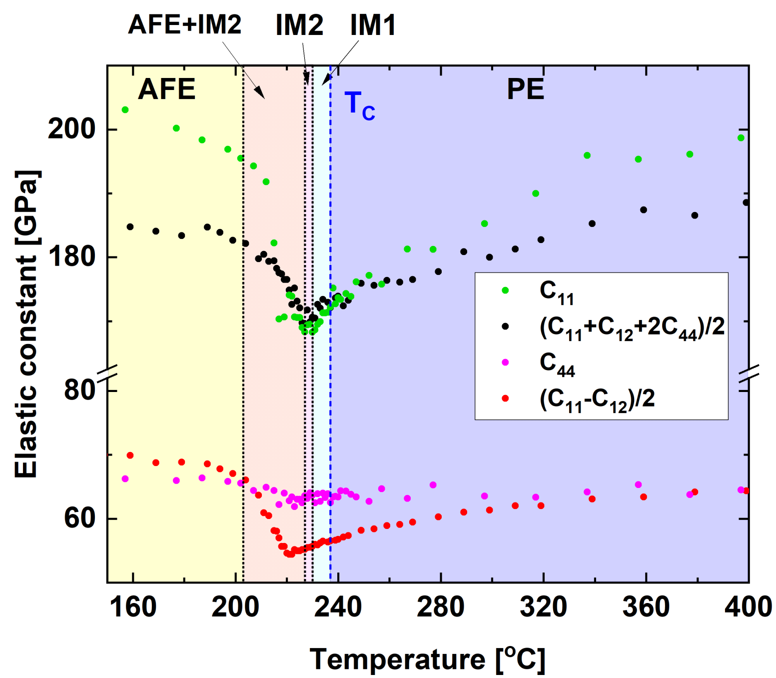

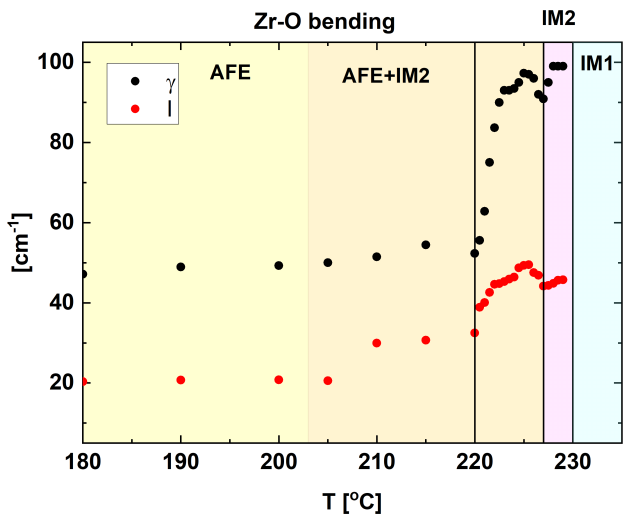

Summary

- Complex structure below and above T_c
- new phase transitions
- Phase coexistence below T_c (AFE + IM2)
- Nb dopant influences polar regions above T_c
- the phase transitions in PZO:Nb are characterised by the simultaneous softening of the zone-centre optical and zone boundary acoustic modes.
- no drastic change in the LA1 mode frequency and the damping was observed at $T_{C.}$ It suggests no modifications of the crystal symmetry at $T_{C.}$
- the phase transition from the PE to IM1 phase is mainly connected with the order-disorder transition mechanism.
- The results demonstrate that T_{BH} does not depend on the existence of defects introduced by doping. It is universal to oxide perovskites and connected with a coupling between the zone-boundary acoustic and zone-centre optic modes.